Neuroestrogens facilitate male-typical behaviors by potentiating androgen receptor signaling in medaka

Yuji Nishiike[1], Shizuku Maki[1], Daichi Miyazoe[1], Kiyoshi Nakasone[1], Yasuhiro Kamei[2], Takeshi Todo[3], Tomoko Ishikawa-Fujiwara[3], Kaoru Ohno[4], Takeshi Usami[4], Yoshitaka Nagahama[4], and Kataaki Okubo[1,*]

[1]Department of Aquatic Bioscience, Graduate School of Agricultural and Life Sciences, The University of Tokyo, Bunkyo, Tokyo 113-8657, Japan

[2]Optics and Bioimaging Facility, Trans-Scale Biology Center, National Institute for Basic Biology, Okazaki, Aichi 444-8585, Japan

[3]Department of Genome Biology, Graduate School of Medicine, Osaka University, Suita, Osaka 565-0871, Japan

[4]Division of Reproductive Biology, National Institute for Basic Biology, Okazaki, Aichi 444-8585, Japan

***Corresponding author:** Kataaki Okubo; Tel: +81-3-5841-5288. Fax: +81-3-5841-5289. E-mail: a-okubo@g.ecc.u-tokyo.ac.jp.

Abstract

In rodents, estrogens aromatized from androgens in the brain, also known as neuroestrogens, are essential for the development of male-typical behaviors. In many other vertebrates including humans and teleost fish, however, androgens facilitate these behaviors directly via the androgen receptor without aromatization into estrogens. Here we report that male medaka fish lacking Cyp19a1b (a subtype of aromatase predominantly expressed in the brain) exhibit severely impaired male-typical mating and aggression, despite elevated brain androgen levels. These phenotypes can be rescued by estrogen administration, indicating that neuroestrogens are pivotal for male-typical behaviors even in non-rodents. Our results further suggest that neuroestrogens facilitate male-typical behaviors by potentiating androgen action in the brain via the direct stimulation of androgen receptor transcription, thereby revealing a previously unappreciated mechanism of action of neuroestrogens. We additionally show that female fish lacking Cyp19a1b are less receptive to male courtship and conversely court other females, highlighting the significance of neuroestrogens in establishing sex-typical behaviors in both sexes.

Keywords: aggression; androgen receptor; aromatase; mating; neuroestrogen

Introduction

Male and female animals exhibit differences in many innate behaviors, such as mating and aggression (1). In vertebrates, these differences are driven primarily by the influence of sex steroid hormones, including estrogens and androgens. Extensive research in rodents has established that estrogens, traditionally considered "female" hormones, are critical for the development of male-typical behaviors (2–4). Specifically, androgens secreted by the testis, both perinatally and in adulthood, are converted to estrogens in the brain by the enzyme aromatase. These brain-derived estrogens, also called neuroestrogens, then act through ESR1, a subtype of the estrogen receptor (ESR), to elicit male-typical behaviors (2–4). This process, originally referred to as the "aromatization hypothesis", is now widely accepted as correct; however, the mechanisms through which neuroestrogens affect male-typical behavior, including the identity of their downstream targets, remain largely elusive (4, 5).

More importantly, the aromatization hypothesis seems to apply to only a limited number of species besides rodents (e.g., some birds such as zebra finches) (6). In other species such as humans, other primates, and teleost fish, testicular androgens facilitate male-typical behaviors directly through the androgen receptor (AR) without aromatization (7–9). Notably, in teleosts, 11-ketotestosterone (11KT), which cannot be aromatized to estrogens, is the primary testicular androgen, and exogenous 11KT effectively induces male-typical courtship and aggression even in females (9–11). Therefore, it is generally assumed that, in teleosts, androgens are solely responsible for male-typical behaviors, while estrogens are dispensable for these behaviors. This is consistent with the recent finding in medaka fish (*Oryzias latipes*) that estrogens act through the ESR subtype Esr2b to prevent females from engaging in male-typical courtship (10).

Interestingly, despite these findings, adult teleost brains have extremely high levels of aromatase activity (100–1000 times higher than in rodent brains), resulting in large amounts of neuroestrogens even in males (12). This observation suggests that neuroestrogens have a vital, but as yet undetermined, role in male teleosts. Most teleost species have two distinct genes encoding aromatase, *cyp19a1a* and *cyp19a1b*, due to a whole-genome duplication that occurred early in teleost evolution (12, 13). These genes have undergone subfunctionalization through the partitioning of tissue-specific expression patterns: *cyp19a1a* is expressed predominantly in the gonad, whereas *cyp19a1b* is expressed in the brain (12, 13).

In the present study, we generated *cyp19a1b*-deficient medaka, in which neuroestrogen synthesis is selectively impaired while gonadal estrogen synthesis remains intact, in order to investigate the impact of neuroestrogens on male behaviors. Contrary to our expectations, the fish showed severely impaired male-typical behaviors, thus revealing the marked behavioral effects of neuroestrogens. Our results further suggest that these effects are mediated by potentiating androgen signaling in behaviorally relevant brain regions.

Results

cyp19a1b-deficient males exhibit severely impaired male-typical mating and aggressive behaviors

We generated a *cyp19a1b*-deficient medaka line from a mutant founder carrying a nonsense mutation in exon 4 of *cyp19a1b* that was identified through screening of the medaka TILLING (targeting-induced local lesions in genomes) library (14) (Fig. S1, A and B). Loss of *cyp19a1b* function in these fish was verified by measuring brain and peripheral levels of sex steroids. As expected, brain estradiol-17β (E2) in both male and female homozygous mutants (*cyp19a1b*$^{-/-}$) was significantly reduced to 16% and 50%, respectively, of the levels in their wild-type (*cyp19a1b*$^{+/+}$) siblings ($P = 0.0037$, males; $P = 0.0092$, females) (Fig. 1, A and B). In males, brain E2 in heterozygotes (*cyp19a1b*$^{+/-}$) was also reduced to 45% of the level in wild-type siblings ($P = 0.0284$) (Fig. 1A). In contrast, peripheral E2 levels were unaltered in both *cyp19a1b*$^{-/-}$ males and females (Fig. S1, C and D), consistent with the expected functioning of Cyp19a1b primarily in the brain. Brain levels of testosterone, as opposed to E2, increased 2.2-fold in *cyp19a1b*$^{-/-}$ males relative to wild-type siblings ($P = 0.0006$) (Fig. 1A). Similarly, brain 11KT levels in *cyp19a1b*$^{-/-}$ males and females increased 6.2- and 1.9-fold, respectively, versus wild-type siblings ($P = 0.0007$, males; $P = 0.0316$, females) (Fig. 1, A and B). Their peripheral 11KT levels also increased 3.7- and 1.8-fold, respectively ($P = 0.0789$, males; $P = 0.0118$, females) (Fig. S1, C and D). These results show that *cyp19a1b*-deficient fish have reduced estrogen levels coupled with increased androgen levels in the brain, confirming the loss of *cyp19a1b* function. They also suggest that the majority of estrogens in the male brain and half of those in the female brain are synthesized locally in the brain.

Next, we investigated the mating behavior of *cyp19a1b*-deficient males (Fig. 1C). The mating behavior of medaka follows a stereotypical pattern, wherein a series of followings, courtship displays, and wrappings by the male leads to spawning (15). Because 11KT, the primary driver of male-typical behaviors in teleosts, was increased in *cyp19a1b*-deficient males, we predicted that these fish would engage more actively in mating. Contrary to this expectation, however, *cyp19a1b*$^{-/-}$ males showed significantly longer latencies to initiate wrappings ($P = 0.0033$ versus *cyp19a1b*$^{+/+}$, $P = 0.0195$ versus *cyp19a1b*$^{+/-}$) and to spawn ($P = 0.0051$ versus *cyp19a1b*$^{+/+}$, $P = 0.0195$ versus *cyp19a1b*$^{+/-}$) (Fig. 1D), suggesting that they are less motivated to mate.

However, no significant differences were evident in latencies to initiate followings and courtship displays (Fig. 1D); therefore, the possibility that *cyp19a1b*-deficient males are less sexually attractive and less preferred by females could not be ruled out. To ascertain whether *cyp19a1b*-deficient males are indeed less motivated to mate, we further tested their mating behavior using *esr2b*-deficient females, which are unreceptive to male courtship (10), as stimulus females (Fig. 1E); this test eliminates the influence of female receptivity, facilitating an exclusive evaluation of male motivation to mate with females (15). We found that *cyp19a1b*$^{-/-}$ males showed significantly longer latencies to initiate followings ($P = 0.0129$ versus *cyp19a1b*$^{+/+}$, $P = 0.0060$ versus *cyp19a1b*$^{+/-}$), courtship displays ($P =$

0.0003 versus *cyp19a1b*$^{+/+}$, $P = 0.0006$ versus *cyp19a1b*$^{+/-}$), and wrapping attempts ($P = 0.0009$ versus *cyp19a1b*$^{+/+}$, $P = 0.0282$ versus *cyp19a1b*$^{+/-}$) (Fig. 1F). In addition, they exhibited significantly fewer courtship displays ($P < 0.0001$ versus both *cyp19a1b*$^{+/+}$ and *cyp19a1b*$^{+/-}$) and wrapping attempts ($P < 0.0001$ versus both *cyp19a1b*$^{+/+}$ and *cyp19a1b*$^{+/-}$) (Fig. 1G). These results thus confirmed that *cyp19a1b*-deficient males are less motivated to mate. In our previous study, we found that *esr2b*-deficient females court females preferentially over males (10). Consistent with that finding, here we observed that 12 of 15 *cyp19a1b*$^{+/+}$ females received courtship displays from the *esr2b*-deficient female, as compared with only 2 of 15 *cyp19a1b*$^{+/+}$ males ($P = 0.0003$) (Fig. 1H). Curiously, we further observed that 8 of 15 *cyp19a1b*$^{-/-}$ males received courtship displays from the *esr2b*-deficient female ($P = 0.0321$ versus *cyp19a1b*$^{+/+}$ males) (Fig. 1H). Perhaps *cyp19a1b*$^{-/-}$ males are misidentified as females by *esr2b*-deficient females because they are reluctant to court or they exhibit some female-like behavior.

Next, we examined the intrasexual aggressive behavior of *cyp19a1b*-deficient males (Fig. 1I). The aggressive behavior of teleosts including medaka consists of five types of behavioral acts: chases, fin displays, circles, strikes, and bites (16). Again, contrary to our expectation, *cyp19a1b*$^{-/-}$ males exhibited all of these aggressive acts less frequently than *cyp19a1b*$^{+/+}$ and/or *cyp19a1b*$^{+/-}$ males, with significant differences observed for chases ($P = 0.0123$ versus *cyp19a1b*$^{+/-}$), fin displays ($P = 0.0214$ versus *cyp19a1b*$^{+/+}$), and bites ($P = 0.0015$ versus *cyp19a1b*$^{+/+}$, $P = 0.0002$ versus *cyp19a1b*$^{+/-}$) (Fig. 1J). These observations demonstrate that *cyp19a1b*-deficient males are less aggressive toward other males.

In tilapia (*Oreochromis niloticus*), depletion of *cyp19a1b* has been reported to cause male infertility due to efferent duct obstruction (17). If this is also the case in medaka, the observed behavioral defects might be secondary to infertility. We therefore investigated the fertilization and hatching success of embryos derived from mating between *cyp19a1b*$^{-/-}$ males and wild-type females. Their fertilization and hatching rates were 88.5% (n = 183) and 93.2% (n = 162), respectively, indicating that *cyp19a1b*-deficient male medaka have normal fertility.

Neuroestrogens facilitate male-typical behaviors probably by stimulating brain AR expression

We considered that the impaired male-typical behaviors of *cyp19a1b*-deficient males might be reasonably attributed to either reduced E2 or increased 11KT in the brain. The latter possibility seemed unlikely because 11KT/AR signaling strongly promotes male-typical behaviors in teleosts (15, 18); therefore, we tested the former possibility by examining whether E2 treatment would rescue the behavioral phenotypes of *cyp19a1b*-deficient males (Fig. 2A). E2 treatment, while having no effect in *cyp19a1b*$^{+/+}$ males (Fig. 2, B and C), significantly shortened the latency to ($P = 0.0005$) and increased the number of ($P = 0.0006$) courtship displays in *cyp19a1b*$^{-/-}$ males (Fig. 2, D and E). These results demonstrated that reduced E2 in the brain was the primary cause of the mating defects, indicating a pivotal role of neuroestrogens in male mating behavior. In contrast, E2 treatment was not effective in restoring aggression in *cyp19a1b*$^{-/-}$ males (Fig. S2A). It is possible that the treatment protocol used may have failed to replicate the estrogenic milieu necessary to induce aggression in males.

We then considered the mechanism by which neuroestrogens facilitate male-typical behaviors. Our previous study showed that exogenous E2 upregulates the expression of a subtype of AR, Ara, in the medaka brain (19; note that Ara was termed Arb in this reference). We therefore hypothesized that neuroestrogens may facilitate male-typical behaviors by stimulating Ara expression and thereby potentiating 11KT/Ara signaling in the brain. To test this hypothesis, we first examined *ara* expression in the brain of *cyp19a1b*-deficient males by in situ hybridization analysis. Expression of *ara* was significantly lower in *cyp19a1b*$^{-/-}$ males than in *cyp19a1b*$^{+/+}$ males in several preoptic and hypothalamic nuclei that are activated upon mating and/or attack in males (15), including the PPa, pPPp, and NVT (P = 0.0134, 0.0372, and 0.0008, respectively) (Fig. 2, F and G; see Table S1 for abbreviations of brain nuclei). We then performed a similar analysis for the other AR subtype, Arb. Expression of *arb* was significantly lower in *cyp19a1b*$^{-/-}$ than in *cyp19a1b*$^{+/+}$ males in other preoptic and hypothalamic nuclei activated upon mating and/or attack (15), including the PMp, aPPp, and NPT (P = 0.0009, 0.0413, and 0.0021, respectively) (Fig. 2, H and I).

Next, to determine whether these reductions in *ara* and *arb* expression in *cyp19a1b*$^{-/-}$ males were the result of reduced brain E2, we tested whether E2 treatment could restore the expression of the two genes. In situ hybridization revealed significantly increased *ara* and *arb* expression in most brain nuclei of E2-treated *cyp19a1b*$^{-/-}$ males as compared with vehicle-treated *cyp19a1b*$^{-/-}$ males (similar results were obtained in *cyp19a1b*$^{+/+}$ males) (Fig. 2, J and K; Fig. S2, B and C; Fig. S3), indicating that the decreased *ara* and *arb* expression in *cyp19a1b*$^{-/-}$ males is attributable to reduced E2 levels. Taken together, these results suggest that neuroestrogens elicit male-typical behaviors by stimulating *ara* and *arb* expression in behaviorally relevant brain regions.

cyp19a1b deficiency impairs behaviorally relevant signaling pathways downstream of ARs

We considered that, if our hypothesis that neuroestrogens facilitate male-typical behaviors by potentiating androgen/AR signaling is correct, then *cyp19a1b*-deficient males should have impaired activation of behaviorally relevant genes that act downstream of ARs. Two neuropeptide genes, *vt* (encoding vasotocin) and *gal* (encoding galanin), have been implicated in male-typical mating and aggressive behaviors in various vertebrates, including medaka and other teleosts (11, 15, 16, 20, 21). In medaka, subsets of neurons in the pNVT and pPMp express *vt* and *gal*, respectively, in an androgen-dependent and hence male-biased manner, and these neurons have been implicated in male-typical behaviors (11, 16, 22). We therefore studied the expression of *vt* and *gal* in the brains of *cyp19a1b*-deficient males.

In situ hybridization revealed that, as expected, expression of *vt* in the pNVT of *cyp19a1b*$^{-/-}$ males was significantly reduced to 18% as compared with *cyp19a1b*$^{+/+}$ males (P = 0.0040), a level comparable to that observed in females (Fig. 3, A and B). In contrast, there were no significant differences between genotypes in other brain nuclei (Fig. 3A). Similarly, expression of *gal* in the pPMp of *cyp19a1b*$^{-/-}$ males was reduced to 43% as compared with *cyp19a1b*$^{+/+}$ males (P = 0.0019), while no significant differences

were observed in other brain nuclei (Fig. 3, C and D). These results demonstrate that *cyp19a1b* deficiency severely impairs the AR-dependent activation of behaviorally relevant *vt* and *gal* expression, suggesting that neuroestrogens play a substantial role in activating AR signaling.

Estrogens directly stimulate the transcription of ARs through ESRs

The above results led us to further explore how neuroestrogens stimulate the expression of *ara* and *arb*. In silico analysis of the medaka *ara* and *arb* loci identified two canonical bipartite estrogen-responsive element (ERE)-like sequences in introns 1 and 2 of *ara* (located at positions +1699 and +2050, respectively, relative to the transcription initiation site) and three in the 5′-flanking region of *arb* (at positions –1272, –2180, and –3327) (Fig. 4, A and B). Thus, neuroestrogens might be able to directly activate the transcription of *ara* and *arb*. To evaluate this likelihood, we conducted in vitro transcriptional activity assays in which luciferase expression was driven by genomic fragments from the *ara* and *arb* loci containing the identified ERE-like sequences.

An assay using the *ara* genomic fragment revealed that E2 dose-dependently increased luciferase activity in the presence of any ESR subtype (Esr1, Esr2a, or Esr2b) (Fig. 4C), suggesting that E2 has the ability to directly activate *ara* transcription through ESRs. The introduction of a point mutation into the ERE-like sequence at position +2050 abolished the E2-induced luciferase activity in the presence of any ESR subtype, while mutation at +1699 had no such effect (Fig. 4D). These results suggest that the ERE at position +2050 is responsible for E2-induced activation of *ara* transcription. Because there is evidence that a single ERE half-site is sufficient to confer E2 responsiveness on several genes (23), we performed the assay using *ara* genomic fragments in which a mutation was introduced in either half-site of the ERE at +2050. E2 induction of luciferase activity was abrogated in both cases (Fig. S4A), suggesting that both ERE half-sites are required to confer estrogen responsiveness on *ara*.

In the assay using the *arb* genomic fragment, E2 also dose-dependently increased luciferase activity in the presence of any ESR subtype (Fig. 4E). The E2-induced increase was completely abolished by point mutation of the ERE-like sequence at position –3327 in the presence of any ESR subtype (Fig. 4F). A similar effect was observed for mutation of the ERE-like sequence at position –1272, but only in the presence of Esr1 and not in the presence of Esr2a or Esr2b (Fig. 4F). These results indicate that E2 can directly stimulate *arb* transcription, primarily through the ERE at –3327. Mutations in either half-site of this ERE eliminated induction by E2 in the presence of Esr2a or Esr2b, but not Esr1 (Fig. S4B), suggesting that both ERE half-sites are required to confer estrogen responsiveness on *arb*. Collectively, these experiments suggest that the transcription of *ara* and *arb* can be directly stimulated by estrogens (including neuroestrogens) via the binding of ESRs to canonical bipartite EREs.

Neuroestrogens stimulate *ara* and *arb* expression in behaviorally relevant brain regions primarily through Esr2a and Esr1, respectively

Next, we investigated whether neuroestrogens can induce *ara* and *arb* expression through ESRs in vivo and, if so, which ESR subtype (Esr1, Esr2a, or Esr2b) mediates this induction. To this end, we

examined *ara* and *arb* expression in the brains of males deficient for each ESR subtype by in situ hybridization. We used previously described *esr1*- and *esr2b*-deficient medaka (10, 24) and generated *esr2a*-deficient medaka using the CRISPR (clustered regularly interspaced short palindromic repeats) / Cas9 (CRISPR-associated protein 9) system. Two independent *esr2a*-deficient lines (Δ8 and Δ4) were established (Fig. S5) and used for subsequent behavioral experiments to ensure the reproducibility of the observed phenotypes.

In $esr1^{+/+}$ and $esr1^{-/-}$ males, *ara* expression was not significantly different between genotypes in any brain nucleus (Fig. S6A), but *arb* expression was significantly lower in $esr1^{-/-}$ than in $esr1^{+/+}$ males in the PMp and aPPp (P = 0.0111 and 0.0376, respectively) (Fig. 5, A and B). This, together with our observation that *arb* expression in these brain nuclei was also significantly lower in $cyp19a1b^{-/-}$ males (Fig. 2H), suggests that neuroestrogens stimulate *arb* expression in these nuclei primarily through Esr1. In support of this notion, double-label in situ hybridization in the wild-type male brain detected neurons coexpressing *arb* and *esr1* in both the PMp and aPPp (Fig. S6B). In $esr2a^{+/+}$ and $esr2a^{-/-}$ male brains (from the Δ8 line), *ara* expression was significantly lower in $esr2a^{-/-}$ than in $esr2a^{+/+}$ males in the PPa, pPPp, and NVT (P = 0.0359, 0.0430, and 0.0178, respectively) (Fig. 5, C and D), while no significant difference was observed in *arb* expression (Fig. S6C). Considering that *ara* expression in these nuclei was also lower in $cyp19a1b^{-/-}$ males (Fig. 2F), neuroestrogens presumably stimulate *ara* expression in these nuclei mainly through Esr2a. This idea was further supported by double-label in situ hybridization, which detected neurons coexpressing *ara* and *esr2a* in the PPa, pPPp, and NVT of wild-type males (Fig. S6D). Examination of $esr2b^{+/+}$ and $esr2b^{-/-}$ male brains showed significantly lower expression of *ara* in the NAT and higher expression of *arb* in the PPa of $esr2b^{-/-}$ males (Fig. S6, E to H); however, no such changes in expression were observed in $cyp19a1b^{-/-}$ males (Fig. 2, F and H). It therefore seems unlikely that Esr2b mediates the effect of neuroestrogens on AR expression. Collectively, these results suggest that neuroestrogens stimulate *ara* and *arb* expression in behaviorally relevant brain regions primarily through Esr2a and Esr1, respectively.

esr1- and *esr2a*-deficient males are, respectively, less motivated to mate and less aggressive

If Esr1 and Esr2a truly mediate the behavioral effects of neuroestrogens through the activation of AR expression, then *esr1*- and *esr2a*-deficient males should exhibit impaired male-typical behaviors. More specifically, given that Esr1 and Esr2a function to activate the expression of *arb* and *ara*, which are responsible for male mating and aggression, respectively (15), *esr1*- and *esr2a*-deficient males should be less motivated to mate and less aggressive, respectively.

To test these ideas, we first evaluated the mating behavior of *esr1*-deficient males using a wild-type female as the stimulus. As expected, $esr1^{-/-}$ males showed a significantly longer latency to initiate followings than $esr1^{+/+}$ males (P = 0.0055) (Fig. S7), suggesting that they are less motivated to mate. This was further confirmed in tests using an *esr2b*-deficient female as the stimulus, where $esr1^{-/-}$ males showed a longer latency to followings and fewer courtship displays than $esr1^{+/+}$ males (P = 0.0426 and

0.0039, respectively) (Fig. 5, E to G). In contrast, no deficits were observed in the mating behavior of *esr2a*$^{-/-}$ males toward wild-type females (Fig. S8, A and B). Although *esr2a*$^{-/-}$ males of the Δ8 line showed a shorter latency to followings than their wild-type siblings in tests using a stimulus *esr2b*-deficient female ($P = 0.0146$) (Fig. 5, H to J), this was not reproduced in the Δ4 line (Fig. S8, C and D). We subsequently assessed aggressive behavior and found no defects in *esr1*$^{-/-}$ males (Fig. 5K). Conversely, *esr2a*$^{-/-}$ males exhibited significantly fewer fin displays ($P = 0.0461$ and 0.0293 for Δ8 and Δ4 lines, respectively) and circles ($P = 0.0446$ and 0.1512 for Δ8 and Δ4 lines, respectively) than their wild-type siblings (Fig. 5L; Fig. S8E), suggesting less aggression. Taken together with the previous finding that *esr2b*-deficient males show no deficits in either mating or aggressive behavior (10), these results suggest that neuroestrogens can promote mating with females by stimulating *arb* expression through Esr1 and can increase aggression toward other males by stimulating *ara* expression through Esr2a. Nonetheless, behavioral deficits in *esr1*- and *esr2a*-deficient males were relatively mild as compared with *cyp19a1b*-deficient males (Fig. 1) and *ara*- and *arb*-deficient males (15), suggesting that a compensatory mechanism may exist between ESR subtypes.

cyp19a1b-deficient females are less receptive to males and instead court other females

Finally, we tested the behavioral impact of *cyp19a1b* deficiency in females. Tests of the mating behavior of *cyp19a1b*$^{-/-}$ females revealed that they had significantly longer latencies to receive the first wrapping from the stimulus male ($P = 0.0018$ versus *cyp19a1b*$^{+/+}$, $P = 0.0117$ versus *cyp19a1b*$^{+/-}$) and to spawn ($P = 0.0015$ versus *cyp19a1b*$^{+/+}$) (Fig. 6, A and B). These results are consistent with a recent study in zebrafish (*Danio rerio*) showing that *cyp19a1b*-deficient females are less receptive to male courtship (25). We further found that the number of courtship displays and wrapping attempts from the male was not increased in *cyp19a1b*$^{-/-}$ females (Fig. 6C), despite their reduced receptivity. This suggests that they are not only less receptive to male courtship but may also actively avoid males, depriving them of mating opportunities. We tested this assumption by measuring the distance between fish, which confirmed that *cyp19a1b*$^{-/-}$ females spent significantly less time near males at distances of 10–20 mm ($P = 0.0438$) and 20–30 mm ($P = 0.0002$) as compared with *cyp19a1b*$^{+/+}$ females (Fig. 6D). We therefore explored the possibility that *cyp19a1b*$^{-/-}$ females may develop a stronger sexual preference for females than for males. In tests of the mating behavior between two females, 4 of 10 *cyp19a1b*$^{-/-}$ females exhibited courtship displays toward the stimulus female, while 0 of 9 *cyp19a1b*$^{+/+}$ females did ($P = 0.0396$) (Fig. 6, E and F). These results demonstrate that *cyp19a1b*-deficient females, having a slightly female-oriented sexual preference, are less receptive to male courtship and, conversely, court other females.

Notably, these behavioral phenotypes of *cyp19a1b*-deficient females, albeit milder, closely resemble those of *esr2b*-deficient females (10). This led us to hypothesize that *cyp19a1b* deficiency prevents female-typical, and induces male-typical, behavioral phenotypes by decreasing estrogen/Esr2b signaling. If correct, *cyp19a1b*-deficient females should be defective in the activation of behaviorally relevant

299 genes that act downstream of Esr2b. In medaka, subsets of neurons in the Vs/Vp and PMm/PMg express
300 *npba* (encoding neuropeptide B) in an estrogen/Esr2b signaling-dependent and hence female-specific
301 manner, and these neurons have been implicated in female sexual receptivity (10, 26, 27). We therefore
302 examined the expression of *npba* in the brains of *cyp19a1b*-deficient females by in situ hybridization.
303 As expected, *npba* expression in the Vs/Vp and PMm/PMg of *cyp19a1b*$^{-/-}$ females was significantly
304 reduced to 33% and 38%, respectively, of that of *cyp19a1b*$^{+/+}$ females (Vs/Vp, $P = 0.0386$; PMm/PMg,
305 $P = 0.0461$) (Fig. 6, G to J). Expression of *esr2b* in these brain nuclei is also estrogen-dependent and
306 female-specific (10, 19); therefore, we tested whether it is also attributable to neuroestrogens. In situ
307 hybridization showed no significant differences in *esr2b* expression between *cyp19a1b*$^{+/+}$ and
308 *cyp19a1b*$^{-/-}$ females in the Vs/Vp and PMm/PMg, although significant differences were seen in the VM,
309 NAT, and NVT (Fig. 6K), suggesting that *esr2b* expression in the brain relies on ovarian estrogens and
310 not on neuroestrogens. Taken altogether, our findings indicate that neuroestrogens contribute
311 substantially to the induction of female-typical, and the prevention of male-typical, behaviors in females
312 by activating estrogen/Esr2b signaling.

Discussion

In this study, we found that male medaka deficient for *cyp19a1b* exhibit severely impaired male-typical mating and aggression. This observation was unexpected because the fish had markedly elevated brain levels of 11KT, the primary driver of male-typical behaviors in teleosts (9, 11). These behavioral deficits were rescued by estrogen administration, indicating that reduced levels of neuroestrogens are the primary cause of the observed phenotypes: in other words, neuroestrogens are pivotal for male-typical behaviors in teleosts. This was also unexpected because, unlike in rodents, where the necessity for neuroestrogens has been codified as the "aromatization hypothesis", neuroestrogens have been regarded as dispensable for male behaviors in many vertebrates, including teleosts (7–9). In addition, the rescue of behavioral phenotypes by estrogen administration in adults suggests that in teleosts, unlike in rodents, neuroestrogen activity in adulthood is sufficient for the execution of male-typical behaviors, while that in early in life is not requisite. Thus, while neuroestrogens are necessary for male behaviors in both rodents and teleosts, the life stages at which they exert their behavioral effects probably differ between these species. Brain aromatase activity in teleosts increases with age and, at adulthood, reaches 100–1000 times that in rodents (9, 12). In contrast, brain aromatase activity in rodents reaches its peak during the perinatal period and thereafter declines with age (28). This variation among species may represent the activation of neuroestrogen synthesis at life stages critical for sexual differentiation of behavior that are unique to each species.

Neuroestrogens serve several functions during the process of sexual differentiation of the mouse brain, including the synthesis of prostaglandin PGE2 and the activation of synaptic and neurodevelopmental genes; however, the specific mechanism whereby neuroestrogens affect male behaviors remains obscure (4, 5, 29). Our findings in medaka indicate that neuroestrogens facilitate male-typical behaviors by potentiating androgen/AR signaling in behaviorally relevant brain regions via the direct stimulation of AR transcription. More specifically, they indicate that neuroestrogens (1) promote mating by stimulating the transcription of *arb* in some preoptic and hypothalamus nuclei via Esr1, and (2) increase aggression by stimulating the transcription of *ara* in other preoptic and hypothalamus nuclei through Esr2a. This model of the mechanism underlying neuroestrogen action would explain the apparent contradiction that, in teleosts, androgens per se elicit male behaviors without aromatization, while neuroestrogens are also critical for these behaviors. Our data also indicate that the two AR genes, *ara* and *arb*, are direct downstream targets of neuroestrogens that mediate male behaviors, only a few of which have been identified thus far. In mice, perinatal neuroestrogens increase *Ar* expression in the bed nucleus of the stria terminalis and preoptic area, two brain regions that have been implicated in male behaviors (30). Recent evidence suggests that ESR1 binds to the regulatory genomic region of *Ar* in these brain regions in mice (29). Given these facts, the idea that neuroestrogens enhance androgen/AR signaling by directly stimulating AR transcription may apply to a wide range of species, including rodents.

Consistent with our results, studies in several teleost species have shown that treatment of males

with an aromatase inhibitor reduces their male-typical behaviors (31–33). Conversely, it has been shown in various teleosts, including medaka, that treatment with exogenous estrogens attenuates male behaviors (34–38). A possible explanation for this discrepancy is that estrogens may either stimulate or suppress male-typical behaviors, depending on their concentration. All studies showing the suppressive effects of exogenous estrogens were conducted at doses higher than those used in the present study or at doses mimicking the levels typical of adult females (39). In addition, our previous study in male medaka showed that high doses of exogenous estrogens induce the expression of *esr2b*, which prevents male-typical mating behavior, in behaviorally relevant brain regions (10). Thus, the development of male behaviors may require moderate neuroestrogen levels that are sufficient to induce the expression of *ara* and *arb*, but not *esr2b*, in the underlying neural circuitry. Another possibility, not mutually exclusive, is that endogenous levels of neuroestrogens are sufficient to motivate males to engage in male-typical behaviors, and therefore exogenous estrogens have no further effect. This possibility is supported by the present observation that estrogen treatment facilitated mating behavior in *cyp19a1b*-deficient males but not in their wild-type siblings. Further studies using *cyp19a1b* mutants from different teleost species are needed to explore these possibilities and to determine whether the findings in medaka hold for other teleosts.

We also found that, as compared with males, females have higher brain levels of estrogens, half of which are synthesized locally in the brain (i.e., neuroestrogens). In many brain nuclei of medaka, expression of *ara* and *arb* is comparable between the sexes or at higher levels in females (19), suggesting that neuroestrogens stimulate AR expression in females as well as in males. This raises the issue of why females do not display male-typical behaviors despite such high brain levels of estrogens and active synthesis of neuroestrogens. Possibly, as mentioned above, high estrogen levels in the female brain may suppress male-typical behaviors by promoting the expression of *esr2b*. Another possibility is that females, despite having abundant ARs in the brain, may lack sufficient amounts of androgen to activate them. This seems highly probable because the treatment of female medaka and other teleosts with 11KT as adults readily induces male-typical behaviors, including courtship and aggression (9–11).

We found that *cyp19a1b*-deficient females are less receptive to male courtship, demonstrating that neuroestrogens influence female, as well as male, mating behavior. This finding is notable when considering that, contrary to mammals and birds, estrogens have been deemed unnecessary for female sexual receptivity in teleosts (40). This notion essentially stems from the observation in several teleost species that exogenous prostaglandin PGF2α is sufficient to restore sexual receptivity in females deprived of ovarian secretions by ovariectomy (41–43). However, we recently challenged it by showing that female medaka deficient for *esr2b* are completely unreceptive to males, and thus estrogens play a critical role in female receptivity (10). The present finding provides a likely explanation for this apparent contradiction, namely, that neuroestrogens, rather than or in addition to ovarian-derived circulating estrogens, may function upstream of PGF2α signaling to mediate female receptivity. This scheme potentially applies to other teleost species because a reduction in female receptivity due to *cyp19a1b* deficiency has been also observed in zebrafish (25).

We further found that *cyp19a1b*-deficient females court other females. To our knowledge, only a few neuronal genes have been identified whose depletion causes females to display male-typical behaviors in vertebrates. These include *trpc2* (encoding a cation channel crucial for olfactory cue-evoked signaling in the vomeronasal organ) and *dmnt3a* (encoding a methyltransferase responsible for de novo DNA methylation) in mice, and *esr2b* in medaka (10, 44, 45). Importantly, deficiency of *cyp19a1b*, unlike that of *esr2b*, did not completely preclude female-typical mating behavior in females, but caused them to exhibit both male- and female-typical mating behaviors. This observation suggests that, in teleosts, the neural circuits mediating these behaviors coexist in the female brain and may be activated simultaneously in the absence of neuroestrogens. This probably also holds true for the male brain, given that *cyp19a1b*-deficient males also showed impaired, but not completely abolished, male-typical behaviors and were actively courted by *esr2b*-deficient females. It is thus plausible that neuroestrogens are required to prevent the simultaneous activation of neural circuits mediating male- and female-typical behaviors, thereby contributing to the mutually exclusive presentation of these behaviors. Such effects of neuroestrogens are likely to be particularly relevant in teleosts, where many species spontaneously undergo sex reversal and their sexual phenotypes, behavioral or otherwise, are highly labile throughout life (46, 47). This may account for the extremely high levels of aromatase activity in the teleost brain.

In summary, we have shown that neuroestrogens promote male-typical behaviors by increasing brain sensitivity to testicular androgens through the stimulation of AR expression. Our findings challenge the prevailing view that neuroestrogens have little effect on male-typical behaviors in species where testicular androgens elicit these behaviors directly without aromatization to neuroestrogens and unveil a previously unappreciated mechanism of neuroestrogen action. Because these species account for the majority of vertebrates, with rodents and some birds being the only known exceptions, the mechanism of neuroestrogen action that we have identified in medaka may be evolutionarily ancient and widely conserved across species.

Materials and Methods

Animals and cell lines

Wild-type d-rR strain medaka and mutant medaka deficient for *cyp19a1b* and *esr2a* (generated in this study), *esr1* (24), and *esr2b* (10) were maintained in a recirculating system at 28ºC on a 14/10-hour light/dark cycle. Three or four times a day, they were fed live brine shrimp and dry food (Otohime; Marubeni Nisshin Feed, Tokyo, Japan). Sexually mature adults (2–6 months) were used for experiments, and tissues were consistently sampled 1–5 hours after lights on. In each experiment, siblings raised under the same conditions were used as the comparison group to control for the effects of genetic diversity and environmental variation. All fish were handled in accordance with the guidelines of the Institutional Animal Care and Use Committee of the University of Tokyo.

HEK293T and HeLa cells used in this study were confirmed to be mycoplasma-free (Biotherapy Institute of Japan, Tokyo, Japan) and authenticated by short tandem repeat profiling (National Institute of Biomedical Innovation, Osaka, Japan).

Generation of mutant medaka

cyp19a1b-deficient medaka were generated essentially as previously described (10). In brief, a TILLING library of 5760 chemically mutagenized medaka (14) was screened for mutations in exons 3, 4, and 5 of *cyp19a1b* by direct sequencing of PCR-amplified fragments. A founder (ID: 57D05) with a nonsense mutation in exon 4 (K105*) was identified (Fig. S1, A and B) and backcrossed to the wild-type d-rR strain for more than six generations to eliminate background mutations. Heterozygous males and females were intercrossed to generate wild-type, heterozygous, and homozygous siblings. All experimental fish were subjected to genotyping by PCR amplification across the mutation, followed by high-resolution melting (HRM) analysis, using the primers and probe listed in Table S2. HRM analysis was performed on the LightCycler 480 System II (Roche Diagnostics, Basel, Switzerland) using the LCGreen Plus dye (BioFire Defense, Salt Lake City, UT).

esr2a-deficient medaka were generated by using the CRISPR/Cas9 system. A CRISPR RNA (crRNA) targeting exon 3 of *esr2a* (Fasmac, Kanagawa, Japan) (Fig. S5A) was injected with trans-activating crRNA (Fasmac) and Cas9 protein (Nippon Gene Co. Ltd., Tokyo, Japan) into the cytoplasm of one- or two-cell stage embryos. The resulting fish were screened for germline mutations by outcrossing to wild-type fish and testing progeny for target site mutations by T7 endonuclease I assay (48) and direct sequencing. Two founders were identified that reproducibly yielded progeny carrying frameshift mutations that eliminated the DNA- and ligand-binding domains of Esr2a: one yielded progeny carrying an 8-bp deletion (Δ8); the other yielded progeny carrying a 4-bp deletion (Δ4) (Fig. S5, A and B). The progeny were intercrossed to obtain wild-type, heterozygous, and homozygous siblings. The genotype of each experimental fish was determined by HRM analysis as described above.

Measurement of sex steroid levels

Brain and peripheral levels of sex steroids were determined by enzyme-linked immunosorbent assay (ELISA) (10). Total lipids were extracted from the brain and peripheral tissues (from the caudal half) of *cyp19a1b*$^{+/+}$, *cyp19a1b*$^{+/-}$, and *cyp19a1b*$^{-/-}$ males and females with chloroform/methanol (2:1, v/v) and purified on a Sep-Pak C18 Plus Light Cartridge (Waters Corporation, Milford, MA). Tissue levels of E2, testosterone, and 11KT were measured by using Estradiol, Testosterone, and 11-Keto Testosterone ELISA kits, respectively (Cayman Chemical Company, Ann Arbor, MI).

Mating behavior test

Mating behavior was tested essentially as previously described (27). In brief, on the day before behavioral testing, each focal fish (*cyp19a1b*-, *esr1*-, and *esr2a*-deficient lines) was placed with a stimulus fish (wild-type females in the tests shown in Fig. 1, C and D, Fig. 6, E and F, Fig. S7, and Fig. S8, A and B; *esr2b*-deficient females in Fig. 1, E to H, Fig. 2, A to E, Fig. 5, E to J, and Fig. S8, C and D; wild-type males in Fig. 6, A to C) in a 2-liter rectangular tank with a perforated transparent partition separating them. The set-up was modified for E2-treated males, which were kept on E2 treatment and not introduced to the test tanks until the day of testing. The partition was removed 1 hour after lights on, and fish were allowed to interact for 30 min while their behavior was recorded with a digital video camera (HC-V360MS, HC-VX985M, or HC-W870M; Panasonic Corporation, Osaka, Japan). The first 15 min of the recording was used to calculate the latency to the first following, courtship display, wrapping, and spawning. The period of interaction/recording was extended to 2 hours in tests of courtship displays received from the stimulus *esr2b*-deficient female and in tests of mating behavior between females, because they take longer to initiate courtship (10). In tests using an *esr2b*-deficient female as the stimulus fish, where the latency to spawn could not be calculated because these fish were unreceptive to males and did not spawn, the sexual motivation of the focal fish was instead assessed by counting the number of courtship displays and wrapping attempts in 30 min. The number of these mating acts was also counted in tests to evaluate the receptivity of females. In tests of mating behavior between two females, the stimulus female was marked with a small notch in the caudal fin to distinguish it from the focal female.

Aggressive behavior test

To test male–male aggressive behavior (16), four males of the same genotype (*cyp19a1b*-, *esr1*-, and *esr2a*-deficient lines) that were unfamiliar with one another were placed together in a test tank 1 hour after lights on. After 1 min of acclimation to the tank, fish were allowed to interact for 15 min while their behavior was video-recorded as described above. The total number of each aggressive act (chase, fin display, circle, strike, and bite) displayed by the four males in the tank was counted manually from the video recordings.

E2 treatment

cyp19a1b$^{+/+}$ and *cyp19a1b*$^{-/-}$ males were treated with 1 ng/ml of E2 (Fujifilm Wako Pure Chemical,

Osaka, Japan) or vehicle (ethanol) alone by immersion in water for 4 days. The mating and aggressive behaviors of males before and after E2 treatment were evaluated as described above. The expression of *ara* and *arb* in the brain of E2- and vehicle-treated males was investigated by single-label in situ hybridization as described below.

Single-label in situ hybridization

Digoxigenin (DIG)-labeled cRNA probes were generated by in vitro transcription using DIG RNA Labeling Mix (Roche Diagnostics), T7 RNA polymerase (Roche Diagnostics), and the following cDNA fragments: *ara*, nucleotide 16–1030 of GenBank NM_001122911 (1015 bp); *arb*, 53–1233 of NM_001104681 (1181 bp); *vt*, 1–845 of NM_001278891 (845 bp); *gal*, 5–533 of LC532140 (529 bp); *npba*, 1–645 of NM_001308979 (645 bp); and *esr2b*, 2080–3288 of XM_020713365 (1209 bp).

Single-label in situ hybridization was essentially done as described (49). In brief, brains dissected from males and females of the *cyp19a1b*-deficient line (analysis of *ara*, *arb*, *vt*, *gal*, *npba*, and *esr2b*) and males of the *esr1*-, *esr2a*-, and *esr2b*-deficient lines (analysis of *ara* and *arb*) were fixed in 4% paraformaldehyde and embedded in paraffin. Serial coronal sections of 10-μm thickness were hybridized with a DIG-labeled probe. Hybridization signal was detected with anti-DIG conjugated to alkaline phosphatase (RRID: AB_514497; Roche Diagnostics) and visualized using 5-bromo-4-chloro-3-indolyl phosphate/nitro blue tetrazolium substrate (Roche Diagnostics). After color development for 15 min (*gal*), 40 min (*npba*), 2 hours (*vt*), or overnight (*ara*, *arb*, and *esr2b*), sections were imaged using a VS120 virtual slide microscope (Olympus, Tokyo, Japan), and the total area of signal in each brain nucleus was calculated using Olyvia software (Olympus). Medaka brain atlases (50, 51) were used to identify brain nuclei.

Transcriptional activity assay

Each full-length coding region of medaka Esr1 (GenBank XM_020714493), Esr2a (NM_001104702), and Esr2b (XM_020713365) cDNA was amplified by PCR and inserted into the expression vector pcDNA3.1/V5-His-TOPO (Thermo Fisher Scientific, Waltham, MA). Each nucleotide sequence of the 5′-flanking region of *ara* and *arb* was retrieved from the Ensembl medaka genome assembly and analyzed for potential canonical ERE-like sequences using Jaspar (version 5.0_alpha) and Match (public version 1.0) with default settings. No ERE-like sequence was detected in *ara*; therefore, the gene body and 3′-flanking region were also analyzed in this case. The transcription initiation site for *ara* and *arb* was determined based on an expressed sequence tag clone deposited in National BioResource Project (NBRP) Medaka (olova36n18) and GenBank NM_001104681, respectively. Medaka bacterial artificial chromosome (BAC) clones containing the *ara* (clone ID: ola1-111G01) and *arb* (ola1-192H15) loci were obtained from NBRP Medaka. A 4530-bp genomic DNA fragment upstream of *ara* exon 3 (comprising 2330 bp of the 5′-flanking region, exon 1, intron 1, exon 2, intron 2, and the first 32 bp of exon 3) was amplified by PCR from the BAC clone, fused to a P2A self-cleaving peptide sequence (52) at the 3′ end, and inserted into the NheI site of the luciferase reporter

vector pGL4.10 (Promega, Madison, WI). Similarly, a 3995-bp fragment upstream of the first methionine codon of *arb* (comprising 3815 bp of the 5′-flanking region and 180 bp of exon1) was PCR-amplified and inserted into pGL4.10. The resulting constructs were transiently transfected into HEK293T (*ara*) or HeLa (*arb*) cells, together with an internal control vector pGL4.74 (Promega) and the Esr1, Esr2a, or Esr2b expression construct using Lipofectamine LTX (Thermo Fisher Scientific). Six hours after transfection, cells were incubated for 18 hours without and with E2 at doses of 10^{-11} M, 10^{-9} M, and 10^{-7} M in Dulbecco's modified Eagle's medium (phenol red-free) containing 5% charcoal/dextran-stripped fetal bovine serum (Cytiva, Marlborough, MA). Luciferase activity was determined using the Dual-Luciferase Reporter Assay System (Promega) on the GloMax 20/20n Luminometer (Promega). All assays were conducted in duplicate or triplicate and repeated independently three times.

Further assays were performed with luciferase reporter constructs carrying point mutations in the ERE-like sequences to identify the ERE responsible for E2 induction of *ara* and *arb* transcription. Each half-site of the responsible ERE-like sequence was mutated into a HindIII recognition site using the PrimeSTAR Mutagenesis Basal Kit (Takara Bio, Shiga, Japan). Transcriptional activity assays with these constructs were done as described above, except that a single dose of E2 (10^{-7} M) was used.

Double-label in situ hybridization

DIG-labeled cRNA probes for *ara* and *arb* were prepared as described above. Fluorescein-labeled cRNA probes for *esr1* and *esr2a* were generated by in vitro transcription using Fluorescein RNA Labeling Mix (Roche Diagnostics), SP6 or T7 RNA polymerase (Roche Diagnostics), and the following cDNA fragments: *esr1*, nucleotides 1694–2781 of XM_020714493 (1088 bp); *esr2a*, 1838–2276 of NM_001104702 plus 763 bp of 3′-untranslated sequence derived from the Ensembl medaka genome assembly (439 bp).

Double-label in situ hybridization was done as described previously (24), with minor modifications. In brief, brains dissected from wild-type males were fixed in 4% paraformaldehyde, embedded in paraffin, and coronally sectioned at 10-µm thickness. Sections were hybridized simultaneously with the DIG-labeled *ara* or *arb* probe and fluorescein-labeled *esr1* or *esr2a* probe. DIG was detected with a mouse anti-DIG antibody (RRID: AB_304362; Abcam, Cambridge, UK) and visualized using the Alexa Fluor 555 Tyramide SuperBoost Kit, goat anti-mouse IgG (Thermo Fisher Scientific); fluorescein was detected with an anti-fluorescein antibody conjugated to horseradish peroxidase (RRID: AB_2737388; PerkinElmer, Waltham, MA) and visualized using the TSA Plus Fluorescein System (PerkinElmer). Cell nuclei were counterstained with DAPI. Fluorescent images were acquired with a Leica TCS SP8 confocal laser scanning microscope (Leica Microsystems, Wetzlar, Germany) and the following excitation/emission wavelengths: 552/620–700 nm (Alexa Fluor 555), 488/495–545 nm (fluorescein), and 405/410–480 nm (DAPI).

Measurement of spatial distances between fish

The distance between the two fish in the test tank was measured as described elsewhere (10). On the day preceding measurement, each focal female (*cyp19a1b*-deficient line) and a stimulus wild-type male were placed together in a 2-liter rectangular tank with a perforated transparent partition separating them. On the following day after lights on, the fish were transferred to a 25-cm (i,d,) cylindrical test tank containing 1.8 L of dechlorinated tap water with a transparent partition separating them. One hour after lights on, the partition was removed and the behavior of the fish was video-recorded for 10 min. Distances between fish were calculated by using UMA Tracker (53).

Statistical analysis

All quantitative data were expressed as mean ± standard error of the mean (SEM). On graphs, individual data points were plotted to indicate the underlying distribution. Behavioral time-series data were analyzed using Kaplan–Meier plots with the inclusion of fish that did not exhibit the given act within the test period.

Statistical analyses were done using GraphPad Prism (GraphPad Software, San Diego, CA). Data between two groups were compared using unpaired two-tailed Student's *t* test. Welch's correction was applied if the *F* test indicated that the variance between groups was significantly different. The Bonferroni–Dunn correction was applied for multiple comparisons between two groups. To compare data among more than two groups, one-way analysis of variance (ANOVA) was performed, followed by either Bonferroni's (comparisons among experimental groups) or Dunnett's (comparisons between control and experimental groups) post hoc test. If the Brown-Forsythe test indicated a significant difference in variance across groups, the data were instead analyzed using the non-parametric Kruskal–Wallis test, followed by Dunn's post hoc test. Differences between Kaplan–Meier curves were tested for significance using the Gehan–Breslow–Wilcoxon test (with Bonferroni's correction for more than two comparisons). Fish that spawned without any courtship display were excluded from the analysis of courtship display because it was not appropriate to treat them either as fish that did not perform courtship displays within the test duration or as fish that performed the first courtship display 0 seconds before spawning. All data points were included in the analyses and no outliers were defined.

593 # Acknowledgments

594

595 We thank NBRP Medaka for providing the BAC clones, managing the TILLING library, and
596 performing artificial insemination; Dr. Yoshihito Taniguchi for constructing the TILLING library; Dr.
597 Masatoshi Nakamoto for recovering the *cyp19a1b* mutant allele; Akira Hirata, Kaoru Furukawa,
598 Tomiko Iba, and Ayu Kuwakubo for assistance with medaka husbandry. This work was supported by
599 the Ministry of Education, Culture, Sports, Science, and Technology (MEXT), Japan (17H06429 to
600 KOk), the Japan Society for the Promotion of Science (JSPS) (21J20634 to YNi and 23H02305 to KOk),
601 and Regional Fish Institute (Get-Research Grant to KOk).

602 # References
603
604 1. N. Zilkha, Y. Sofer, Y. Kashash, T. Kimchi, The social network: neural control of sex differences
605 in reproductive behaviors, motivation, and response to social isolation. *Curr. Opin. Neurobiol.* **68**,
606 137–151 (2021).
607 2. S. Ogawa, S. Tsukahara, E. Choleris, N. Vasudevan, Estrogenic regulation of social behavior and
608 sexually dimorphic brain formation. *Neurosci. Biobehav. Rev.* **110**, 46–59 (2020).
609 3. S. Tsukahara, M. Morishita, Sexually dimorphic formation of the preoptic area and the bed nucleus
610 of the stria terminalis by neuroestrogens. *Front. Neurosci.* **14**, 797 (2020).
611 4. M. M. McCarthy, Neural control of sexually dimorphic social behavior: connecting development
612 to adulthood. *Annu. Rev. Neurosci.* **46**, 321–339 (2023).
613 5. M. M. McCarthy, B. M. Nugent, K. M. Lenz, Neuroimmunology and neuroepigenetics in the
614 establishment of sex differences in the brain. *Nat. Rev. Neurosci.* **18**, 471–484 (2017).
615 6. J. Balthazart, New concepts in the study of the sexual differentiation and activation of reproductive
616 behavior, a personal view. *Front. Neuroendocrinol.* **55**, 100785 (2019).
617 7. J. Thornton, J. L. Zehr, M. D. Loose, Effects of prenatal androgens on rhesus monkeys: a model
618 system to explore the organizational hypothesis in primates. *Horm. Behav.* **55**, 633–645 (2009).
619 8. J. Bakker, The role of steroid hormones in the sexual differentiation of the human brain. *J.*
620 *Neuroendocrinol.* **34**, e13050 (2022).
621 9. K. Okubo, Y. Nishiike, T. Fleming, Y. Kikuchi, T. Hiraki-Kajiyama, "Sex steroid regulation of
622 male- and female-typical mating behaviors in teleost fish" in *Spectrum of Sex*, M. Tanaka, M.
623 Tachibana, Eds. (Springer Nature, 2022), pp. 111–133.
624 10. Y. Nishiike, D. Miyazoe, R. Togawa, K. Yokoyama, K. Nakasone, M. Miyata, Y. Kikuchi, Y. Kamei,
625 T. Todo, T. Ishikawa-Fujiwara, K. Ohno, T. Usami, Y. Nagahama, K. Okubo, Estrogen receptor 2b
626 is the major determinant of sex-typical mating behavior and sexual preference in medaka. *Curr.*
627 *Biol.* **31**, 1699–1710.e6 (2021).
628 11. Y. Kawabata-Sakata, S. Kanda, K. Okubo, Male-specific vasotocin expression in the medaka
629 tuberal hypothalamus: androgen dependence and probable role in aggression. *Mol. Cell.*
630 *Endocrinol.* **580**, 112101 (2024).
631 12. N. Diotel, T. D. Charlier, C. Lefebvre d'Hellencourt, D. Couret, V. L. Trudeau, J. C. Nicolau, O.
632 Meilhac, O. Kah, E. Pellegrini, Steroid transport, local synthesis, and signaling within the brain:
633 roles in neurogenesis, neuroprotection, and sexual behaviors. *Front. Neurosci.* **12**, 84 (2018).
634 13. Y. Nagahama, T. Chakraborty, B. Paul-Prasanth, K. Ohta, M. Nakamura, Sex determination,
635 gonadal sex differentiation, and plasticity in vertebrate species. *Physiol. Rev.* **101**, 1237–1308
636 (2021).
637 14. Y. Taniguchi, S. Takeda, M. Furutani-Seiki, Y. Kamei, T. Todo, T. Sasado, T. Deguchi, H. Kondoh,
638 J. Mudde, M. Yamazoe, M. Hidaka, H. Mitani, A. Toyoda, Y. Sakaki, R. H. A. Plasterk, E. Cuppen,
639 Generation of medaka gene knockout models by target-selected mutagenesis. *Genome Biol.* **7**,

R116 (2006).

15. Y. Nishiike, K. Okubo, The decision of male medaka to mate or fight depends on two complementary androgen signaling pathways. *bioRxiv* doi: 10.1101/2024.01.10.574747 (2024).
16. J. Yamashita, A. Takeuchi, K. Hosono, T. Fleming, Y. Nagahama, K. Okubo, Male-predominant galanin mediates androgen-dependent aggressive chases in medaka. *eLife* **9**, e59470 (2020).
17. X. Zhang, Q. Min, M. Li, X. Liu, M. Li, D. Wang, Mutation of *cyp19a1b* results in sterile males due to efferent duct obstruction in Nile tilapia. *Mol. Reprod. Dev.* **86**, 1224–1235 (2019).
18. Y. Ogino, S. Ansai, E. Watanabe, M. Yasugi, Y. Katayama, H. Sakamoto, K. Okamoto, K. Okubo, Y. Yamamoto, I. Hara, T. Yamazaki, A. Kato, Y. Kamei, K. Naruse, K. Ohta, H. Ogino, T. Sakamoto, S. Miyagawa, T. Sato, G. Yamada, M. E. Baker, T. Iguchi, Evolutionary differentiation of androgen receptor is responsible for sexual characteristic development in a teleost fish. *Nat. Commun.* **14**, 1428 (2023).
19. T. Hiraki, A. Takeuchi, T. Tsumaki, B. Zempo, S. Kanda, Y. Oka, Y. Nagahama, K. Okubo, Female-specific target sites for both oestrogen and androgen in the teleost brain. *Proc. R. Soc. B* **279**, 5014–5023 (2012).
20. S. Yokoi, T. Okuyama, Y. Kamei, K. Naruse, Y. Taniguchi, S. Ansai, M. Kinoshita, L. J. Young, N. Takemori, T. Kubo, H. Takeuchi, An essential role of the arginine vasotocin system in mate-guarding behaviors in triadic relationships of medaka fish (*Oryzias latipes*). *PLoS Genet.* **11**, e1005009 (2015).
21. J. A. Tripp, I. Salas-Allende, A. Makowski, A. H. Bass, Mating behavioral function of preoptic galanin neurons is shared between fish with alternative male reproductive tactics and tetrapods. *J. Neurosci.* **40**, 1549–1559 (2020).
22. Y. Kawabata, T. Hiraki, A. Takeuchi, K. Okubo, Sex differences in the expression of vasotocin/isotocin, gonadotropin-releasing hormone, and tyrosine and tryptophan hydroxylase family genes in the medaka brain. *Neuroscience* **218**, 65–77 (2012).
23. C. M. Klinge, Estrogen receptor interaction with estrogen response elements. *Nucleic Acids Res.* **29**, 2905–2919 (2001).
24. T. Fleming, M. Tachizawa, Y. Nishiike, A. Koiwa, Y. Homan, K. Okubo, Estrogen-dependent expression and function of secretogranin 2a in female-specific peptidergic neurons. *PNAS Nexus* **2**, pgad413 (2023).
25. K. Shaw, M. Therrien, C. Lu, X. Liu, V. L. Trudeau, Mutation of brain aromatase disrupts spawning behavior and reproductive health in female zebrafish. *Front. Endocrinol.* **14**, 1225199 (2023).
26. T. Hiraki, K. Nakasone, K. Hosono, Y. Kawabata, Y. Nagahama, K. Okubo, Neuropeptide B is female-specifically expressed in the telencephalic and preoptic nuclei of the medaka brain. *Endocrinology* **155**, 1021–1032 (2014).
27. T. Hiraki-Kajiyama, J. Yamashita, K. Yokoyama, Y. Kikuchi, M. Nakajo, D. Miyazoe, Y. Nishiike, K. Ishikawa, K. Hosono, Y. Kawabata-Sakata, S. Ansai, M. Kinoshita, Y. Nagahama, K. Okubo, Neuropeptide B mediates female sexual receptivity in medaka fish, acting in a female-specific but

reversible manner. *eLife* **8**, e39495 (2019).

28. E. D. Lephart, A review of brain aromatase cytochrome P450. *Brain Res. Rev.* **22**, 1–26 (1996).
29. B. Gegenhuber, M. V. Wu, R. Bronstein, J. Tollkuhn, Gene regulation by gonadal hormone receptors underlies brain sex differences. *Nature* **606**, 153–159 (2022).
30. S. A. Juntti, J. Tollkuhn, M. V. Wu, E. J. Fraser, T. Soderborg, S. Tan, S.-I. Honda, N. Harada, N. M. Shah, The androgen receptor governs the execution, but not programming, of male sexual and territorial behaviors. *Neuron* **66**, 260–272 (2010).
31. S. L. E. Hallgren, M. Linderoth, K. H. Olsén, Inhibition of cytochrome p450 brain aromatase reduces two male specific sexual behaviours in the male Endler guppy (*Poecilia reticulata*). *Gen. Comp. Endocrinol.* **147**, 323–328 (2006).
32. L. S. Huffman, L. A. O'Connell, H. A. Hofmann, Aromatase regulates aggression in the African cichlid fish *Astatotilapia burtoni*. *Physiol. Behav.* **112**, 77–83 (2013).
33. C. Jalabert, L. Quintana, P. Pessina, A. Silva, Extra-gonadal steroids modulate non-breeding territorial aggression in weakly electric fish. *Horm. Behav.* **72**, 60–67 (2015).
34. M. Bayley, J. R. Nielsen, E. Baatrup, Guppy sexual behavior as an effect biomarker of estrogen mimics. *Ecotoxicol. Environ. Saf.* **43**, 68–73 (1999).
35. A. M. Bell, Effects of an endocrine disrupter on courtship and aggressive behaviour of male three-spined stickleback, *Gasterosteus aculeatus*. *Anim. Behav.* **62**, 775–780 (2001).
36. R. Bjerselius, K. Lundstedt-Enkel, H. Olsén, I. Mayer, K. Dimberg, Male goldfish reproductive behaviour and physiology are severely affected by exogenous exposure to 17β-estradiol. *Aquat. Toxicol.* **53**, 139–152 (2001).
37. Y. Oshima, I. J. Kang, M. Kobayashi, K. Nakayama, N. Imada, T. Honjo, Suppression of sexual behavior in male Japanese medaka (*Oryzias latipes*) exposed to 17β-estradiol. *Chemosphere* **50**, 429–436 (2003).
38. D. Martinović, W. T. Hogarth, R. E. Jones, P. W. Sorensen, Environmental estrogens suppress hormones, behavior, and reproductive fitness in male fathead minnows. *Environ. Toxicol. Chem.* **26**, 271–278 (2007).
39. D. Kayo, Y. Oka, S. Kanda, Examination of methods for manipulating serum 17β-Estradiol (E2) levels by analysis of blood E2 concentration in medaka (*Oryzias latipes*). Gen Comp. Endocrinol. **285**, 113272 (2020).
40. A. Munakata, M. Kobayashi, Endocrine control of sexual behavior in teleost fish. *Gen. Comp. Endocrinol.* **165**, 456–468 (2010).
41. N. E. Stacey, Effects of indomethacin and prostaglandins on the spawning behaviour of female goldfish. *Prostaglandins* **12**, 113–126 (1976).
42. M. Kobayashi, N. Stacey, Prostaglandin-induced female spawning behavior in goldfish (*Carassius auratus*) appears independent of ovarian influence. *Horm. Behav.* **27**, 38–55 (1993).
43. S. A. Juntti, A. T. Hilliard, K. R. Kent, A. Kumar, A. Nguyen, M. A. Jimenez, J. L. Loveland, P. Mourrain, R. D. Fernald, A neural basis for control of cichlid female reproductive behavior by

716 prostaglandin F2α. *Curr. Biol.* **26**, 943–949 (2016).
717 44. T. Kimchi, J. Xu, C. Dulac, A functional circuit underlying male sexual behaviour in the female
718 mouse brain. *Nature* **448**, 1009–1014 (2007).
719 45. B. M. Nugent, C. L. Wright, A. C. Shetty, G. E. Hodes, K. M. Lenz, A. Mahurkar, S. J. Russo, S.
720 E. Devine, M. M. McCarthy, Brain feminization requires active repression of masculinization via
721 DNA methylation. *Nat. Neurosci.* **18**, 690–697 (2015).
722 46. B. Capel, Vertebrate sex determination: evolutionary plasticity of a fundamental switch. *Nat. Rev.*
723 *Genet.* **18**, 675–689 (2017).
724 47. H. Liu, E. V. Todd, P. M. Lokman, M. S. Lamm, J. R. Godwin, N. J. Gemmell, Sexual plasticity: a
725 fishy tale. *Mol. Reprod. Dev.* **84**, 171–194 (2017).
726 48. H. J. Kim, H. J. Lee, H. Kim, S. W. Cho, J.-S. Kim, Targeted genome editing in human cells with
727 zinc finger nucleases constructed via modular assembly. *Genome Res.* **19**, 1279–1288 (2009).
728 49. Y. Kawabata-Sakata, Y. Nishiike, T. Fleming, Y. Kikuchi, K. Okubo, Androgen-dependent sexual
729 dimorphism in pituitary tryptophan hydroxylase expression: relevance to sex differences in
730 pituitary hormones. *Proc. R. Soc. B* **287**, 20200713 (2020).
731 50. R. Anken, F. Bourrat, *Brain Atlas of the Medaka fish* (INRA Editions, 1998).
732 51. Y. Ishikawa, M. Yoshimoto, H. Ito, A brain atlas of a wild-type inbred strain of the medaka, *Oryzias*
733 *latipes*. *Fish Biol. J. Medaka* **10**, 1–26 (1999).
734 52. J. H. Kim, S. R. Lee, L. H. Li, H. J. Park, J. H. Park, K. Y. Lee, M. K. Kim, B. A. Shin, S. Y. Choi,
735 High cleavage efficiency of a 2A peptide derived from porcine teschovirus-1 in human cell lines,
736 zebrafish and mice. *PLoS One* **6**, e18556 (2011).
737 53. O. Yamanaka, R. Takeuchi, UMATracker: an intuitive image-based tracking platform. *J. Exp. Biol.*
738 **221**, jeb182469 (2018).

Figures

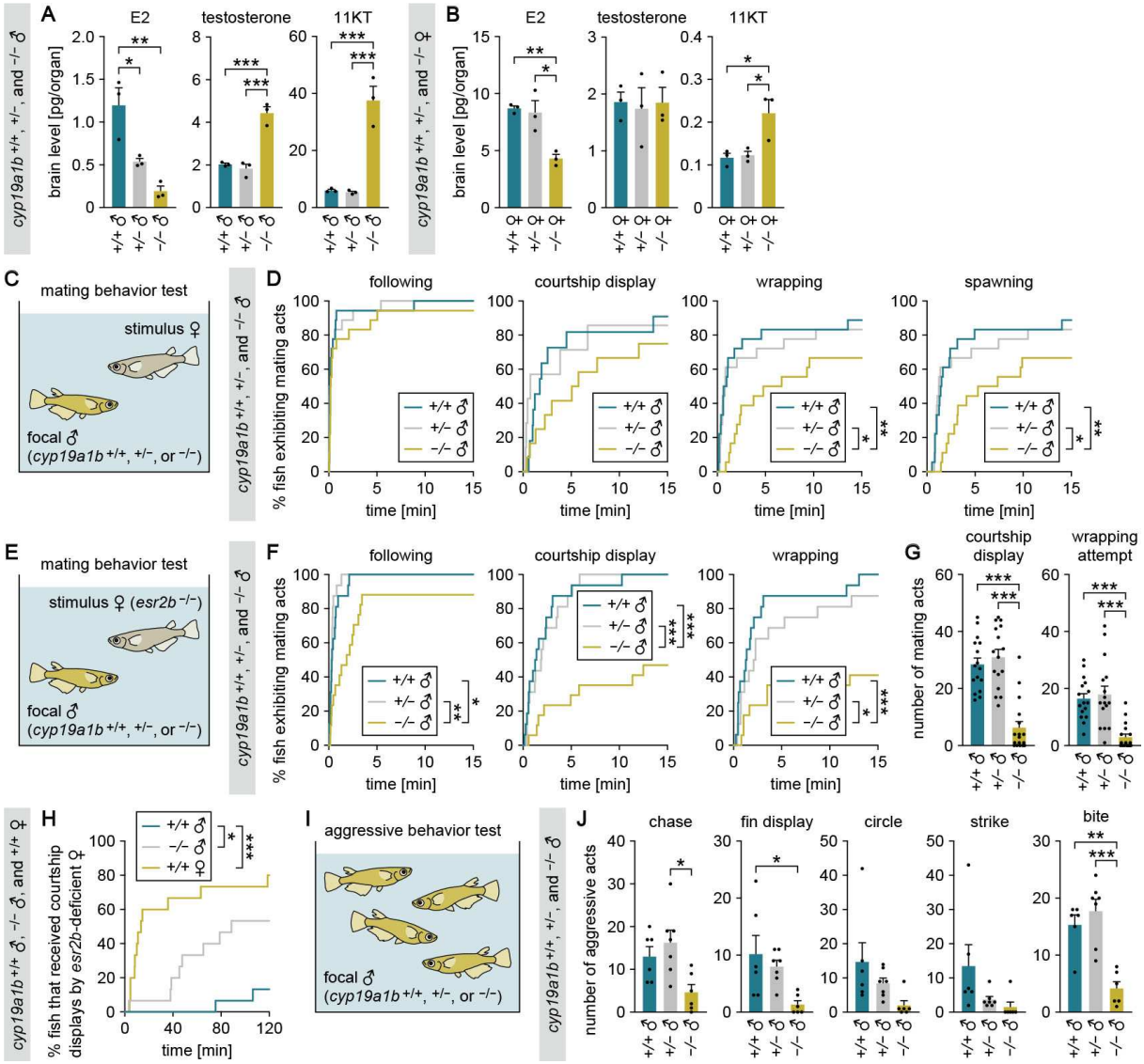

Fig. 1 *cyp19a1b*-deficient males exhibit severely impaired male-typical mating and aggressive behaviors.

(**A** and **B**) Levels of E2, testosterone, and 11KT in the brain of adult *cyp19a1b*$^{+/+}$, *cyp19a1b*$^{+/-}$, and *cyp19a1b*$^{-/-}$ males (A) and females (B) (n = 3 per genotype and sex). (**C**) Set-up for testing the mating behavior of *cyp19a1b*$^{+/+}$, *cyp19a1b*$^{+/-}$, and *cyp19a1b*$^{-/-}$ males. (**D**) Latency of *cyp19a1b*$^{+/+}$, *cyp19a1b*$^{+/-}$, and *cyp19a1b*$^{-/-}$ males (n = 18 per genotype) to initiate each mating act toward the stimulus female. (**E**) Set-up for testing mating behavior using an *esr2b*-deficient female as the stimulus. (**F**) Latency of *cyp19a1b*$^{+/+}$, *cyp19a1b*$^{+/-}$, and *cyp19a1b*$^{-/-}$ males (n = 16, 15, and 17, respectively) to initiate each mating act toward the *esr2b*-deficient female. (**G**) Number of each mating act performed. (**H**) Latency of *cyp19a1b*$^{+/+}$ and *cyp19a1b*$^{-/-}$ males and *cyp19a1b*$^{+/+}$ females (n = 15 each) to receive courtship displays from the *esr2b*-deficient female. (**I**) Set-up for testing aggressive behavior among grouped males. (**J**) Total number of each aggressive act observed among *cyp19a1b*$^{+/+}$, *cyp19a1b*$^{+/-}$, or

755 *cyp19a1b*$^{-/-}$ males in the tank (n = 6, 7, and 5, respectively). Statistical differences were assessed by
756 Bonferroni's or Dunn's post hoc test (A, B, G, and J) and Gehan-Breslow-Wilcoxon test with
757 Bonferroni's correction (D, F, and H). Error bars represent SEM. *$P < 0.05$, **$P < 0.01$, ***$P < 0.001$.

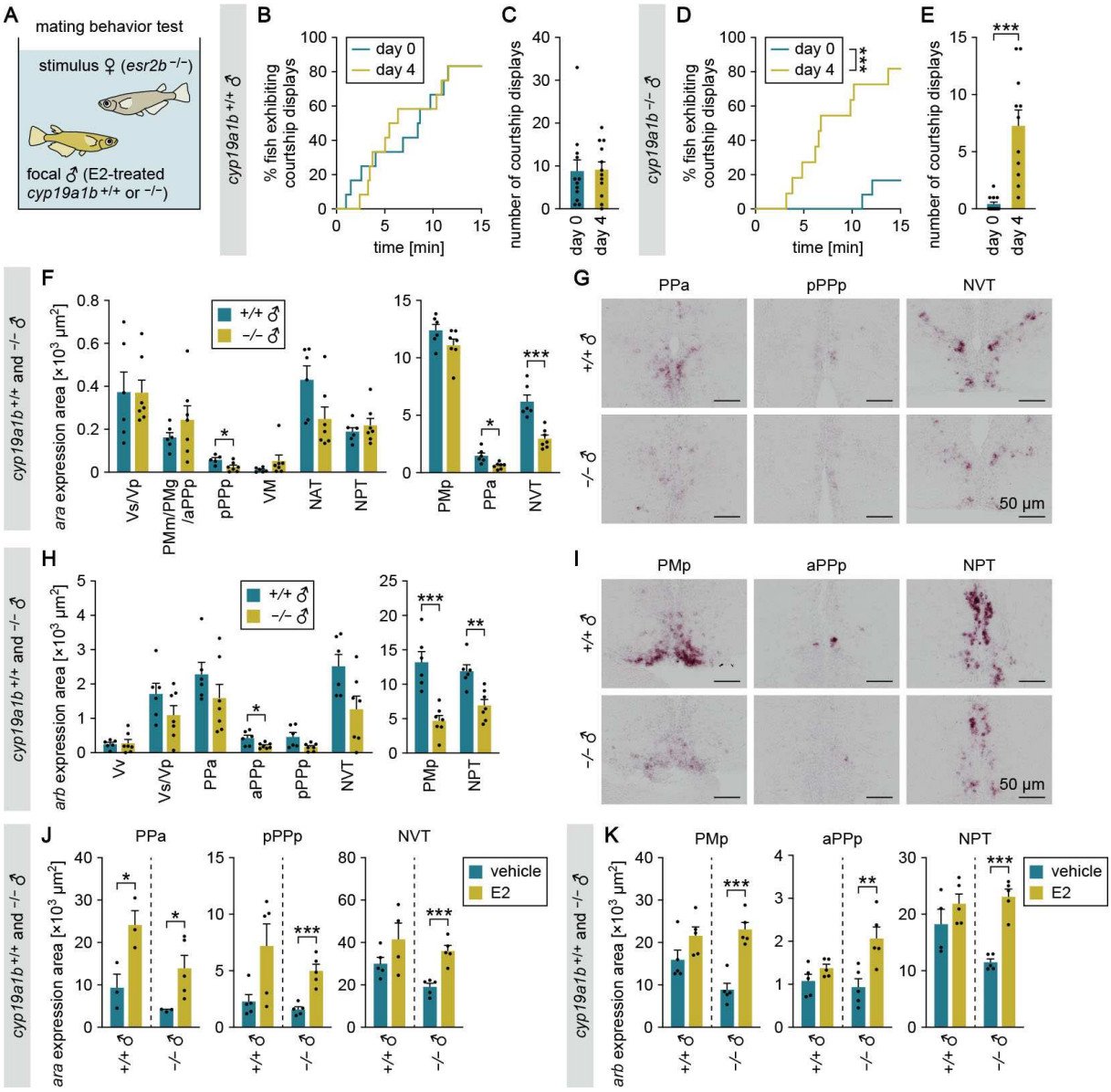

Fig. 2 Neuroestrogens facilitate male-typical behaviors probably by stimulating brain AR expression.

(**A**) Set-up for testing the mating behavior of E2-treated *cyp19a1b*$^{+/+}$ and *cyp19a1b*$^{-/-}$ males. (**B**) Latency of *cyp19a1b*$^{+/+}$ males (n = 12) to initiate courtship displays toward the stimulus female before (day 0) and after (day 4) E2 treatment. (**C**) Number of courtship displays performed by *cyp19a1b*$^{+/+}$ males. (**D**) Latency of *cyp19a1b*$^{-/-}$ males (n = 12) to initiate courtship displays before (day 0) and after (day 4) E2 treatment. (**E**) Number of courtship displays performed by *cyp19a1b*$^{-/-}$ males. (**F**) Total area of *ara* expression signal in each brain nucleus of *cyp19a1b*$^{+/+}$ (n = 6 except for pPPp, where n = 5) and *cyp19a1b*$^{-/-}$ (n = 7) males. The data are displayed in two graphs for visual clarity. (**G**) Representative images of *ara* expression in the PPa, pPPp, and NVT. (**H**) Total area of *arb* expression signal in each brain nucleus of *cyp19a1b*$^{+/+}$ (n = 6) and *cyp19a1b*$^{-/-}$ (n = 7 except for NVT, where n = 6) males. The data are displayed in two graphs for visual clarity. (**I**) Representative images of *arb* expression in the PMp, aPPp, and NPT. (**J**) Total area of *ara* expression signal in the PPa, pPPp, and NVT of *cyp19a1b*$^{+/+}$

and *cyp19a1b*$^{-/-}$ males treated with vehicle alone or E2 (n = 5 per group except for NVT of E2-treated *cyp19a1b*$^{+/+}$ males, where n = 4; and PPa of vehicle-treated *cyp19a1b*$^{+/+}$, E2-treated *cyp19a1b*$^{+/+}$, and vehicle-treated *cyp19a1b*$^{-/-}$ males, where n = 3). (**K**) Total area of *arb* expression signal in the PMp, aPPp, and NPT of *cyp19a1b*$^{+/+}$ and *cyp19a1b*$^{-/-}$ males treated with vehicle alone or E2 (n = 5 per group except for NPT of vehicle-treated *cyp19a1b*$^{+/+}$ males, where n = 4). Scale bars represent 50 μm. For abbreviations of brain nuclei, see Table S1. Statistical differences were assessed by Gehan-Breslow-Wilcoxon test (B and D) and unpaired *t* test, with Welch's correction where appropriate (C, E, F, H, J, and K). Error bars represent SEM. **P* < 0.05, ***P* < 0.01, ****P* < 0.001.

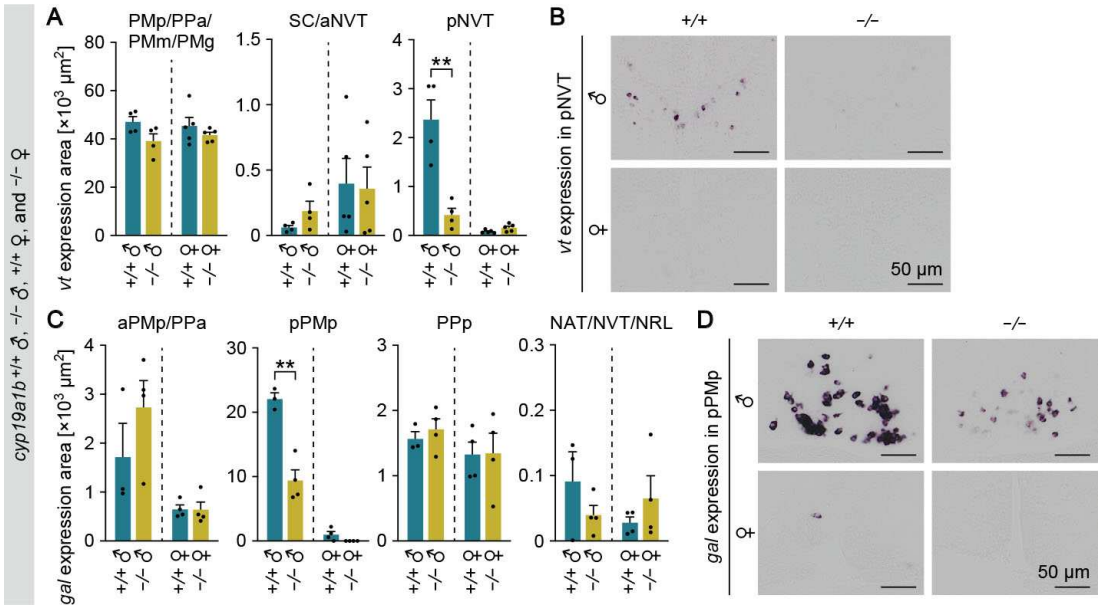

Fig. 3 *cyp19a1b* deficiency impairs behaviorally relevant signaling pathways downstream of ARs.

(**A**) Total area of *vt* expression signal in the PMp/PPa/PMm/PMg, SC/aNVT, and pNVT of *cyp19a1b*$^{+/+}$ and *cyp19a1b*$^{-/-}$ males and females (n = 4 and 5 per genotype for males and females, respectively). (**B**) Representative images of *vt* expression in the pNVT. (**C**) Total area of *gal* expression signal in the aPMp/PPa, pPMp, PPp, and NAT/NVT/NRL of *cyp19a1b*$^{+/+}$ and *cyp19a1b*$^{-/-}$ males and females (n = 4 except for *cyp19a1b*$^{+/+}$ males, where n = 3). (**D**) Representative images of *gal* expression in the pPMp. Scale bars represent 50 µm. For abbreviations of brain nuclei, see Table S1. Statistical differences were assessed by unpaired *t* test, with Welch's correction where appropriate (A and C). Error bars represent SEM. $^{**}P < 0.01$.

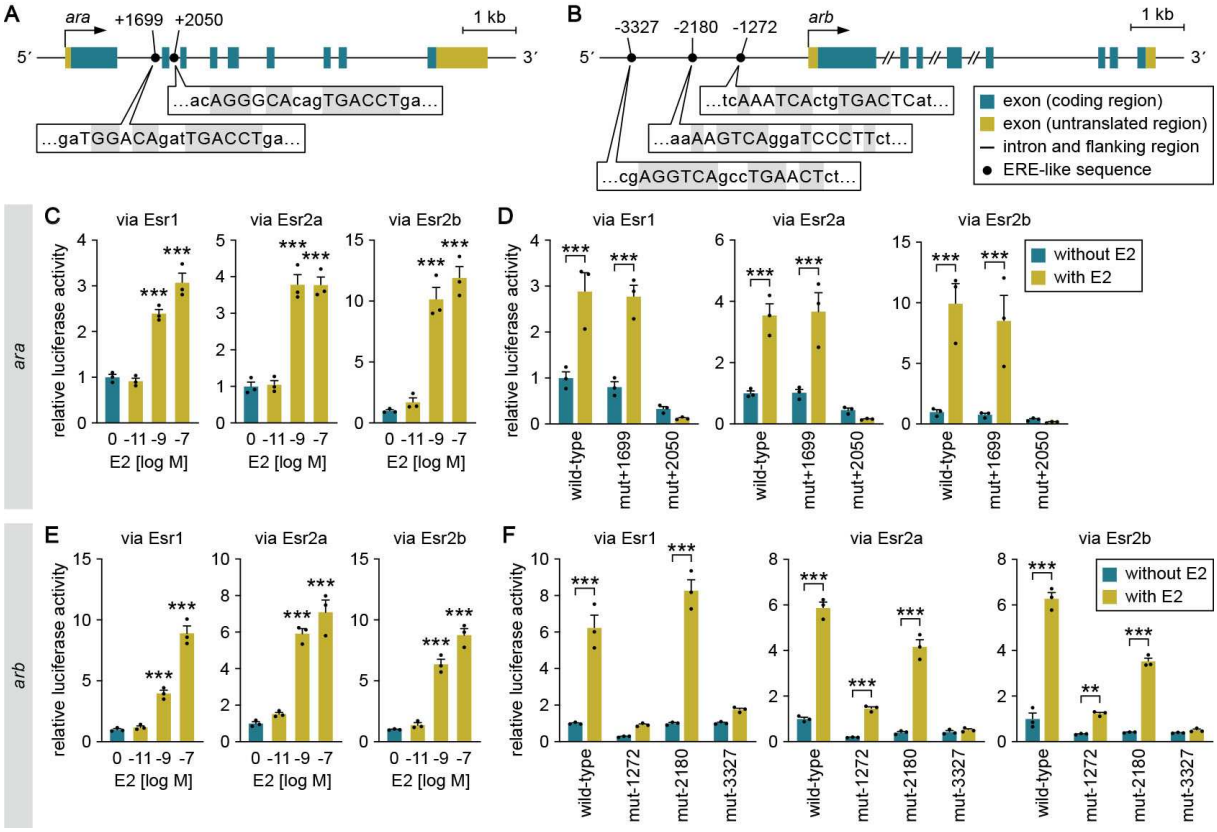

Fig. 4 Estrogens directly stimulate the transcription of ARs through ESRs.

(**A** and **B**) Schematic of *ara* (A) and *arb* (B) loci showing the location of the canonical bipartite ERE-like sequences. Bent arrows mark the transcription initiation sites. Nucleotides of the ERE-like sequences are denoted by capital letters, and those identical to the consensus ERE (AGGTCAnnnTGACCT) are gray-shaded. (**C**) Ability of E2 to directly activate *ara* transcription. Cultured cells were transfected with a luciferase reporter construct containing a genomic fragment upstream of exon 3 of *ara*, together with an Esr1, Esr2a, or Esr2b expression construct. The cells were stimulated with different concentrations of E2 and luciferase activity was measured. (**D**) Effect of mutations in the ERE-like sequences on the E2-induced activation of *ara* transcription. Cultured cells were transfected with a wild-type luciferase construct or a construct carrying a mutation in the ERE-like sequence at position +1699 (mut+1699) or +2050 (mut+2050), together with an Esr1, Esr2a, or Esr2b expression construct. The cells were stimulated with or without E2, and luciferase activity was measured. (**E**) Ability of E2 to directly activate *arb* transcription. The assay described in C was performed with a luciferase construct containing a genomic fragment upstream of the first methionine codon of *arb*. (**F**) Effect of mutations in the ERE-like sequences on the E2-induced activation of *arb* transcription. The assay described in D was performed with luciferase constructs each carrying a mutation in the ERE-like sequence at position –1272 (mut-1272), –2180 (mut-2180), or –3327 (mut-3327). Values are expressed as a fold change relative to a control without E2 stimulation (C and E) or a control using the wild-type construct without E2 stimulation (D and F). Statistical differences were assessed by Dunnett's post hoc test (C and E) and unpaired *t* test with Bonferroni–Dunn correction (D and F). Error bars represent SEM.

815 $^{**}P < 0.01$; $^{***}P < 0.001$.

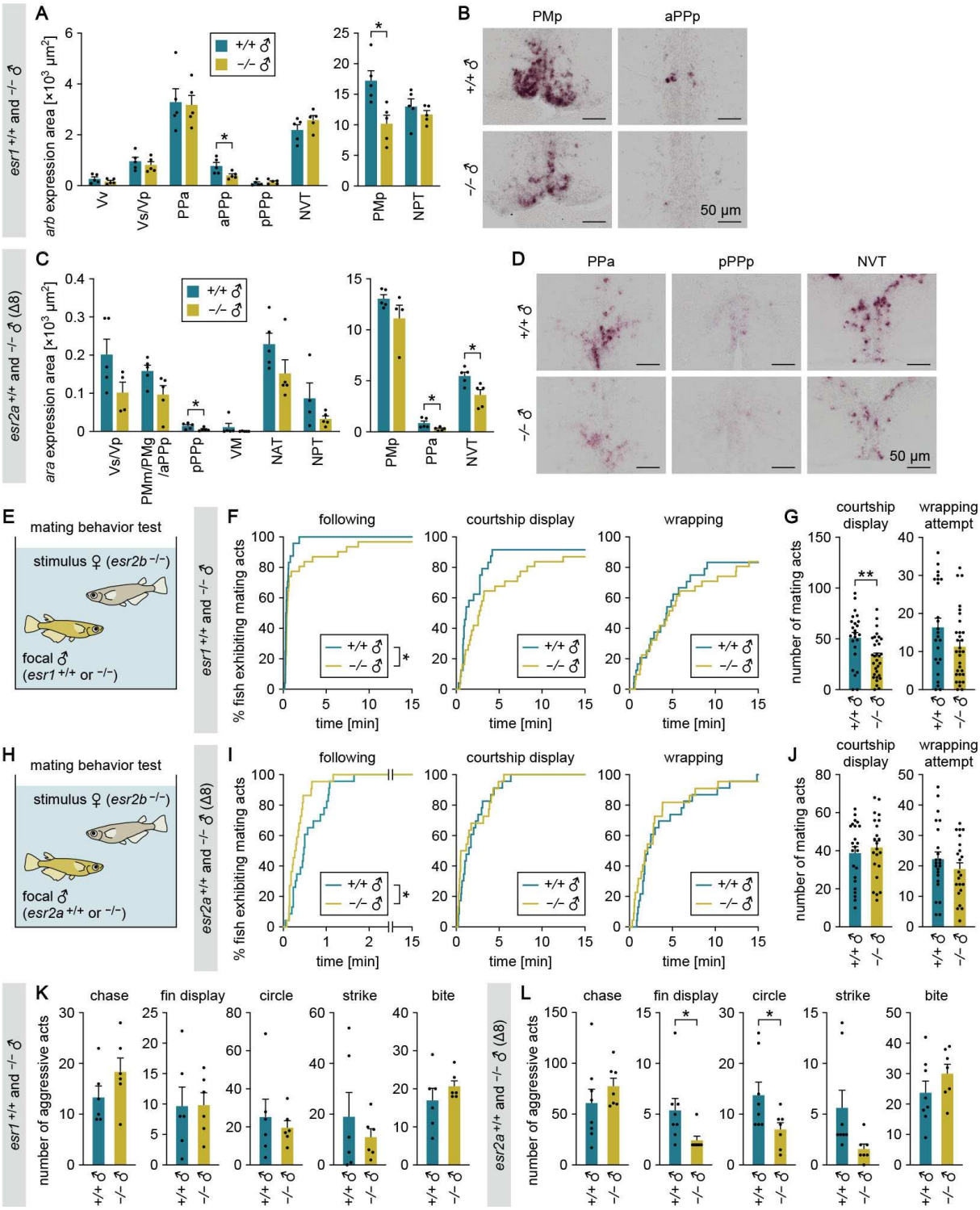

Fig. 5 Neuroestrogens stimulate *ara* and *arb* expression in behaviorally relevant brain regions primarily through Esr2a and Esr1, respectively.

(**A**) Total area of *arb* expression signal in each brain nucleus of *esr1*$^{+/+}$ and *esr1*$^{-/-}$ males (n = 5 per genotype). The data are displayed in two graphs for visual clarity. (**B**) Representative images of *arb* expression in the PMp and aPPp. (**C**) Total area of *ara* expression signal in each brain nucleus of *esr2a*$^{+/+}$ and *esr2a*$^{-/-}$ males (Δ8 line; n = 5 per genotype except for NPT of *esr2a*$^{+/+}$ males and Vs/Vp and PMp

of *esr2a*$^{-/-}$ males, where n = 4). The data are displayed in two graphs for visual clarity. (**D**) Representative images of *ara* expression in the PPa, pPPp, and NVT. (**E**) Set-up for testing the mating behavior of *esr1*$^{+/+}$ and *esr1*$^{-/-}$ males using an *esr2b*-deficient female as the stimulus. (**F**) Latency of *esr1*$^{+/+}$ and *esr1*$^{-/-}$ males (n = 24 and 31, respectively) to initiate each mating act toward the stimulus female. (**G**) Number of each mating act performed. (**H**) Set-up for testing the mating behavior of *esr2a*$^{+/+}$ and *esr2a*$^{-/-}$ males using an *esr2b*-deficient female as the stimulus. (**I**) Latency of *esr2a*$^{+/+}$ and *esr2a*$^{-/-}$ males (Δ8 line; n = 23 and 22, respectively) to initiate each mating act toward the stimulus female. (**J**) Number of each mating act performed. (**K** and **L**) Total number of each aggressive act observed among *esr1*$^{+/+}$ or *esr1*$^{-/-}$ males (n = 6 per genotype) (K) and among *esr2a*$^{+/+}$ or *esr2a*$^{-/-}$ males (Δ8 line; n = 8 and 7, respectively) (L) in the tank. Scale bars represent 50 μm. For abbreviations of brain nuclei, see Table S1. Statistical differences were assessed by unpaired *t* test, with Welch's correction where appropriate (A, C, G, J, K, and L) and Gehan-Breslow-Wilcoxon test (F and I). Error bars represent SEM. **P* < 0.05, ***P* < 0.01.

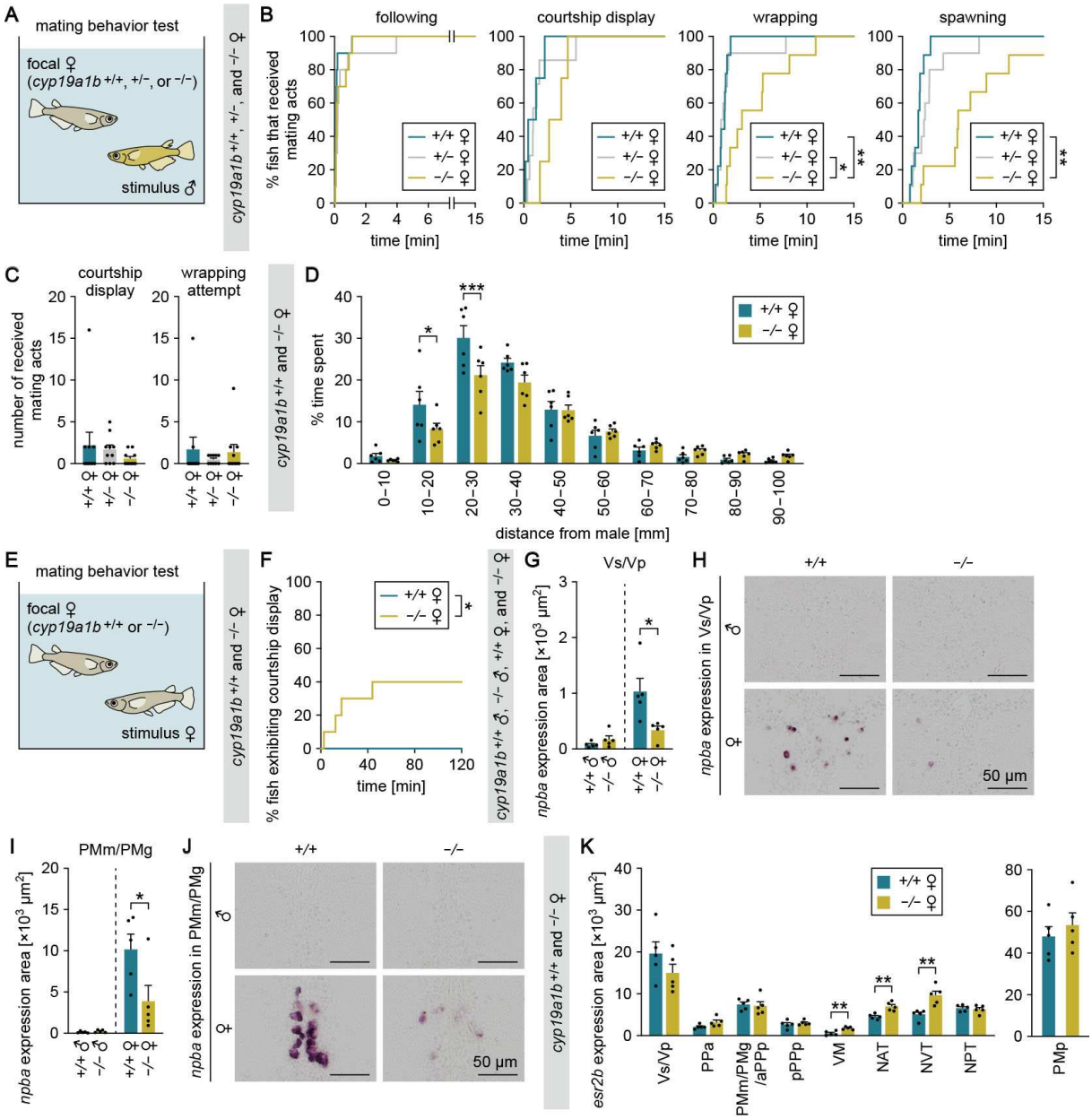

Fig. 6 *cyp19a1b*-deficient females are less receptive to males and instead court other females.

(**A**) Set-up for testing the mating behavior of *cyp19a1b*$^{+/+}$, *cyp19a1b*$^{+/-}$, and *cyp19a1b*$^{-/-}$ females. (**B**) Latency of *cyp19a1b*$^{+/+}$, *cyp19a1b*$^{+/-}$, and *cyp19a1b*$^{-/-}$ females (n = 10 per genotype) to receive each mating act from the stimulus male. (**C**) Number of each mating act received. (**D**) Percentage of time *cyp19a1b*$^{+/+}$ and *cyp19a1b*$^{-/-}$ females (n = 6 per genotype) spent at different distances from the stimulus male. (**E**) Set-up for testing the mating behavior of *cyp19a1b*$^{+/+}$ and *cyp19a1b*$^{-/-}$ females toward a stimulus female. (**F**) Latency of *cyp19a1b*$^{+/+}$ (n = 9) or *cyp19a1b*$^{-/-}$ (n = 10) females to initiate courtship displays toward the stimulus female. (**G** and **H**) Total area (G) and representative images (H) of *npba* expression signal in the Vs/Vp of *cyp19a1b*$^{+/+}$ and *cyp19a1b*$^{-/-}$ males and females (n = 5 per genotype and sex). (**I** and **J**) Total area (I) and representative images (J) of *npba* expression signal in the

PMm/PMg of *cyp19a1b*$^{+/+}$ and *cyp19a1b*$^{-/-}$ males and females (n = 5 per genotype and sex). (**K**) Total area of *esr2b* expression signal in each brain nucleus of *cyp19a1b*$^{+/+}$ or *cyp19a1b*$^{-/-}$ females (n = 5 per genotype). The data are displayed in two graphs for visual clarity. Scale bars represent 50 μm. For abbreviations of brain nuclei, see Table S1. Statistical differences were assessed by Gehan-Breslow-Wilcoxon test, with Bonferroni's correction where appropriate (B and F), Bonferroni's post hoc test (C), unpaired *t* test with Bonferroni–Dunn correction (D), and unpaired *t* test, with Welch's correction where appropriate (G, I, and K). Error bars represent SEM. **P* < 0.05, ***P* < 0.01, ****P* < 0.001.